

Lawrence Berkeley National Laboratory

Lawrence Berkeley National Laboratory

Title

Heterogeneous seepage at the Nopal I natural analogue site, Chihuahua, Mexico

Permalink

<https://escholarship.org/uc/item/03r3955x>

Author

Dobson, P.F.

Publication Date

2011-10-01

Peer reviewed

Heterogeneous seepage at the Nopal I natural analogue site, Chihuahua, Mexico

Patrick F. Dobson*¹, Teamrat A. Ghezzehei², Paul J. Cook¹,

J. Alfredo Rodríguez³, Lourdes Villalba⁴, and Rodrigo de la Garza⁴

¹Earth Sciences Division, Lawrence Berkeley National Laboratory, Berkeley, CA 94720;

²School of Natural Sciences, University of California, Merced, Merced, CA 95343;

³Centro de Investigación sobre Sequía, Instituto de Ecología, Aldama, Chihuahua, Mexico (now at World Wildlife Fund, Chihuahua, Chihuahua, Mexico)

⁴Facultad de Ingeniería, Universidad Autónoma de Chihuahua, Nuevo Campus Universitario, Chihuahua, Chihuahua, México.

*Corresponding author (pfdobson@lbl.gov; tel. 1-510-486-5373; fax. 1-510-486-5686)

Abstract

The subject of this report is seepage occurring in an adit at the Nopal I uranium mine in Chihuahua, Mexico, a natural analogue site used to evaluate processes controlling the mobilization and transport of radionuclides. An instrumented seepage collection system and local automated weather station permit direct correlation between local precipitation events and seepage. Field observations recorded between April 2005 and December 2006 indicate that seepage is highly heterogeneous with respect to time, location, and quantity. Seepage, precipitation, and fracture data were used to test two hypotheses: 1) that fast flow seepage is triggered by large precipitation events, and 2) that an increased abundance of fractures and/or fracture intersections leads to higher seepage volumes. A few zones in the back adit recorded elevated seepage volumes immediately following large (>20 mm/day) precipitation events, with transit times of less than 4 hours through the 8 m thick rock mass. In most locations, there is a 1-6 month time lag between the onset of the rainy season and seepage, with longer times observed for the front adit. There is a less clear-cut relation between fracture abundance and seepage volume; processes such as evaporation and surface flow along the ceiling may also influence seepage.

Keywords: fractured rocks, unsaturated zone, seepage, Mexico

1. Introduction

The primary objectives of the Peña Blanca natural analogue study are to evaluate processes governing the transport of radionuclides from the Nopal I uranium deposit into the surrounding environment and to compare behavior predicted from flow and transport models with field observations. The Peña Blanca system has numerous similarities to the formerly proposed geologic repository of nuclear waste at Yucca Mountain, making it a good analogue for evaluating flow and transport processes (e.g., Murphy 2002; Murphy et al. 2002; Simmons and Stuckless 2010; Levy et al. 2011). Similarities include:

- Thick (>200 m) unsaturated zone
- Host rock consisting of welded rhyolitic ash-flow tuffs
- Semiarid climate with low infiltration rates
- Basin and Range structural setting
- Orebody mineralogy similar to spent nuclear fuel

The goal of the seepage study at the Nopal I mine is to characterize the nature of fluid flow within the unsaturated zone, which can then be used to provide input to flow and transport models (e.g., Saulnier and Statham 2006) and to evaluate radionuclide mobility and transport within the UZ (e.g., Ku et al. 2009). This study consists of evaluating seepage rates and volumes using a high spatial resolution collection system, with a focus on two key aspects of seepage: 1) correlating seepage with seasonal precipitation events, and 2) evaluating the link between primary seepage locations with the observed fracture network at the Nopal I site. These data can be used to develop numerical models that capture the observed variations in seepage.

1.1. Study site

The Nopal I uranium deposit, located ~50 km NE of Chihuahua, Chihuahua, Mexico in the Sierra Peña Blanca (Fig. 1), is hosted by two rhyolitic ash-flow tuff units, the Nopal Formation (44 Ma) and the Coloradas Formation (Reyes-Cortés 2002). The ore deposit is exposed at the ground surface with visible U mineralization over an area of 18 by 30 m; the orebody extends to a depth of ~100 m (Pearcy et al. 1995). The deposit was actively mined in the 1970s and 1980s, but is currently abandoned. As part of the mining activities, a number of benches and adits were constructed. The benches represent horizontal

surfaces with exposed bedrock where infiltration occurs. The +10 level bench was the subject of a detailed fracture study conducted by Percy et al. (1995) and Reyes-Cortés (1997). An adit on the +00 m level of the mine intersects the orebody and goes beneath the exposed +10 m bench; this adit is where the seepage collectors for this study are deployed (Fig. 2).

Three wells were drilled in 2003 around the Nopal I deposit down to the water table to provide stratigraphic information, determine the water table depth, and permit sampling of the saturated zone water (Dobson et al. 2008). The water table is located at a depth of ~220 m below the +10 m bench, thus indicating that the Nopal I uranium orebody is located entirely within the vadose zone. The well PB-1, located immediately adjacent to the +00 level adit, was cored, providing good stratigraphic control. The portion of the +00 level adit where seepage collectors were deployed is located in the lower portion of the Nopal Formation ash-flow tuff, just above the contact with the basal vitrophyre. Geochemical studies of water samples obtained from the adit and nearby wells were conducted to evaluate the transport of radionuclides at the Nopal I site (Ku et al. 2009; Goldstein et al. 2010; Levy et al. 2011).

1.2. Previous studies

Prior mapping and characterization of the Nopal I site (Percy et al. 1995; Prikryl et al. 1997; Reyes-Cortés 1997) demonstrated that the distribution of U outside of the main orebody is concentrated along mineralized fractures, suggesting that fluid flow through fractures is the primary mechanism for transport of radionuclides away from the orebody. Stable isotope and ion probe analyses of U minerals at the Nopal I deposit indicate that U mobilization has occurred repeatedly over the past 30 Ma, and at relatively low (<80°C) temperatures (Fayek et al. 2006; Calas et al. 2008). Analysis of U isotope ratios and U abundance in seepage waters collected from the Nopal I +00 adit indicates that fluid transport of U is non-steady state and intermittent in nature (Ku et al. 2009). To develop more complex models describing the flow and transport of radionuclides from the uranium orebody into the surrounding environment, a better understanding of fluid flow within the thick unsaturated zone at Nopal I is needed.

Previous workers proposed a similar seepage study at the Nopal I site (Green and Rice 1995), but only limited seepage information was collected at the site prior to our study. Pickett and Murphy (1999) report major anion and cation concentration and Th and U isotope data for two seepage samples collected from the back adit of the Nopal I mine. The samples were collected using ~2 m square plastic

sheets that were connected with funnels and tubing to collection bottles. Rapid infiltration into the +00 adit was reported to occur after a succession of rainstorms in September of 1995, but the total seepage volumes and sampling duration for these samples were not given. Simmons et al. (2002) reported U isotopic data from a series of seepage samples collected from the Nopal adit using the plastic sheet collection method. Goldstein et al. (2006, 2010) and Ku et al. (2009) interpreted the observed uranium isotope mixing relations from collected seepage waters to indicate that samples from the back adit have lower U dissolution rates and shorter water-rock interaction times relative to those from the front adit area of the Nopal I mine. All of these earlier studies were limited by a lack of constraints on seepage sampling and the timing of discrete rainfall events.

2. Methods

A rudimentary water collection system consisting of plastic sheeting and wooden frames had been installed by previous investigators within the +00 m adit of the Nopal I mine to collect water that infiltrated from the +10 m level and seeped into the adit (Pickett and Murphy 1999; Simmons et al. 2002). This collection system was upgraded in April of 2005, when the plastic collection tarps were replaced with a 240-bottle collection system to collect spatially discretized samples and reduce potential water losses resulting from evaporation. The new seepage capture system, similar to that utilized by Trautz and Wang (2002) at Yucca Mountain, consists of four aluminum racks deployed within different portions of the +00 adit (Fig. 2). Each rack has a 12 by 5 array of Lexan compartments (30.5 cm x 30 cm by 15 cm deep) that are mounted on top of the rack near the adit ceiling. The rows of collection compartments are numbered 1 through 48 starting from the innermost compartment in the back adit, and the columns are labeled A through E from left to right (see Fig. 2b). The compartments are individually connected by Tygon tubing to 125 ml Nalgene bottles (Fig. 3). This system was further enhanced in November of 2005, when instrumentation was added to six selected collector sites within the back adit (locations 3C, 8C, 18A, 24C, 30D, and 34E) to measure seepage rates continuously within 1.905 cm ID by 70 cm high Plexiglas collection columns fitted with absolute pressure transducers (Setra) (Fig. 3). These locations were chosen to provide spatial variability (two sites per frame in the back adit) as well as to provide more detailed characterization of low-seepage and high-seepage areas as identified from seepage measurements made between April and November of 2005.

In November 2005, sensors were installed within the back adit to monitor changes in temperature, atmospheric pressure, and relative humidity. The pressure transducers (Setra) and temperature-relative humidity sensors (Vaisala) were connected to a battery-powered datalogger (Campbell Scientific Inc., Logan, UT), with measurements recorded every two hours. The absolute pressure transducers (Setra) were replaced with gauge pressure transducers (Druck) in June of 2006. Temperature, atmospheric pressure, relative humidity, and radon levels were also monitored while working in the adit (AlphaGUARD, Genitron Instruments GmbH, Frankfurt am Main, Germany).

An automated weather station (Vantage Pro 2, Davis Instruments Inc., Hayward, CA) was installed at the site in March of 2006 (at a location ~65 WSW of the adit collectors) to permit direct correlation of local precipitation events with seepage. Meteorological data, including temperature, barometric pressure, precipitation, wind speed and direction, were recorded for each two hour interval and downloaded during each visit to the site, up to the end of the study in December of 2006.

Prior to the installation of the seepage collection trays, the ceiling of the adit was photographed, with the frames for the trays providing points of reference. Most of the fractures in the adit were observed to be steeply dipping. Using field observations and a photomosaic constructed from these photographs, a detailed map of the fracture network over the areas, where the seepage trays were located, was constructed (Fig. 4) and compared with fracture maps for the corresponding surface region on the +10 bench above (Pearcy et al. 1995; Reyes-Cortés 1997). Based on the adit fracture map, the total length of fractures within each seepage tray zone was determined, along with the number of fracture intersections. To examine the effects of larger fractures, the lengths of a subset of larger fractures were also determined.

The surface of the adit roof was quite irregular. Measured distances between the top of the collection trays (located ~1.8 m above the floor of the adit) to the adit ceiling ranged from 0 to 89 cm. The front adit collectors are located only 2–5 meters away from the margin of the uranium orebody, whereas the back adit collectors are a bit more distant (7–21 m) from the deposit (Fig. 2b).

Seepage amounts were monitored at each collection location during visits to the site in September and November of 2005 and January, March, June, August, and December of 2006 to determine the timing and amounts of seepage within the adit. For sites with bottles, the water levels in

the collection bottles were noted during each visit by marking the water level on the bottle and comparing water levels with a calibrated bottle, thus permitting a volumetric estimate of seepage volumes between each site visit. Bottles were routinely collected (usually when they had accumulated more than 40 ml of water) and replaced with new bottles beginning with the November 2005 visit. Collected bottles were used to determine seepage volumes at the corresponding marks more accurately (± 2 ml) in the laboratory, and selected seepage water samples were chosen for isotopic and chemical analyses.

3. Results

3.1. Rainfall data

Rainfall in central Chihuahua is seasonal, with most precipitation occurring during the summer monsoon period (June through September). Historical average monthly rainfall data (1961-1972) from the Los Pozos weather station of the Servicio Meteorológico Nacional located about 5 km ESE of Nopal I indicates an annual total rainfall of 300 mm. Rainfall data obtained during March – December of 2006 from the automated weather station installed at the Nopal I site is consistent with this trend, with little rainfall occurring in the spring and significant rain events during the summer months (Fig. 5). There were three major (> 20 mm/day) precipitation events and 14 minor (5-10 mm) events observed during the 2006 rainy season.

The +10 level above the +00 adit was excavated when the uranium mine was active, and consists of flat exposed bedrock (Fig. 2a). The area was cleared of debris during the fracture mapping conducted by Southwest Research Institute in the 1990s (Percy et al. 1995; Reyes-Cortés 1997), and since that time, only small amounts of grasses and sagebrush have taken root in the back (NW) portion of this area. Precipitation falling on this surface tends to pool in small depressions on the excavated bedrock surface and infiltrates along fractures and into the pore spaces of the exposed bedrock. Runoff is presumed to be minimized by the lack of slope on the mined surface, and the lack of vegetation likely minimizes transpiration losses. However, the absence of soil on the +10 level could lead to rapid evaporation of any standing pools of water in this arid climate.

3.2. Seepage data

Using the data recorded from the individual seepage collection bottles and the instrumented seepage columns, two types of seepage data are available. For the majority of the seepage collection

sites, seepage amounts are averaged over the time between site visits, thus providing a time resolution of several months between measurements (Fig. 6). These results do not permit correlation of seepage with individual rainfall events, but do provide important insights into the overall temporal and detailed spatial distribution of seepage within the adit. Detailed temporal seepage information is available from the six instrumented seepage columns, where continuous seepage data were recorded, thus permitting direct correlation between rainfall events and changes in seepage behavior (Fig. 7).

Both collector types (bottles and instrumented columns) were limited by the total storage volume. When the volume of the containers (~135 ml) or columns (~340 ml) was exceeded, in most cases, water leaked out of the connection between the containers and the Nalgene tubing. In several instances, this connection did not leak, and large volumes of water were preserved in the Lexan trays, which have an additional capacity of ~6750 ml. Thus, for instances where the containers or columns were full, the measured values represent a minimum seepage volume for that collection interval.

Comparison of the timing of seepage from the instrumented collectors in the Nopal I adit with precipitation events (Fig. 7) indicates that some locations (collectors 3C, 8C, and 18A) had large increases in seepage immediately following the 3 major rain events (> 20 mm/day) on July 6, August 12, and September 2, 2006. Other locations (collectors 24B, 30D, 34E) had little or no seepage during the onset of the summer rainy season, and experienced slight increases in seepage rates several months after the initiation of rainfall. As seen in the bulk seepage pattern (Fig. 7), there is a large variability in seepage within each collection frame, as some 30.5 cm × 30 cm collectors have captured more than 6 L of water over the deployment period, while nearby collectors within the same frame captured very little (<150 ml) seepage water. In general, seepage within the back adit area occurred earlier than in the front adit region, where water infiltrating from the summer rainfall did not reach the adit until November to January, about 6 months after the start of the rainy season.

3.3. Fracture data

Fractures were mapped for the area above the seepage frames to permit a systematic evaluation of the effect of fracture density and fracture intersections on seepage volumes (Fig. 4). Almost all of the seepage trays have fractures above them, but as mentioned earlier, there were large differences in the amounts of seepage observed throughout the adit.

The fracture network observed in the adit was compared to the fractures mapped by Percy et al. (1995) and Reyes-Cortés (1997) for the corresponding overlying area on the exposed +10 level (Fig. 4). While the overall density and pattern of fractures is similar for the two areas, there are few features that can be directly correlated between the two surfaces. There is a fault, having a strike and dip of N37E, 81SE, that was mapped cutting through the middle portion of the third seepage frame area. This prominent feature is also seen (with its trace displaced slightly to the NW) in the fracture map of the +10 surface.

4. Discussion

Fluid flow through unsaturated fractured rock has been the subject of numerous field and modeling studies (e.g., Shimojima et al. 1993; Davidson et al. 1998; Liu et al. 1998; Finsterle 2000; Bagtzoglou and Cesano 2007a). At Yucca Mountain, fast flow paths along fault zones were postulated to explain the presence of bomb-pulse tritium and ^{36}Cl at depths of up to 300 m below the ground surface (e.g., Flint et al. 2001a; Campbell et al. 2003). Mineral precipitation in fractures provides additional evidence for flow and transport through a portion of the fracture network at Yucca Mountain (Paces et al. 1998). Field and modeling studies at the Stripa mine in Sweden (Abelin et al. 1991 a, b) revealed that water flow rates observed within a drift appeared to be higher for regions of the drift that had a higher frequency of fracture intersections. However, there was no apparent correlation between the abundance of fractures (which are ubiquitous in nature) and seepage rates within the Stripa drifts, suggesting that some fractures played a more important role in flow and transport within the fractured granite.

The difference between the amount of infiltration that occurs at the surface and the rate of seepage occurring within an underground opening is in part controlled by the effectiveness of the capillary barrier in diverting flow around the opening. High volumes of infiltration triggered by large precipitation events may help exceed the seepage threshold of fractures, which is determined by the capability of individual fractures to hold water by capillary forces. Channelized flow within a fracture network may both focus flow (and seepage), and can also lead to flow diversion around a drift or underground opening (Houseworth et al. 2003). The relation between seepage, precipitation, evaporation, condensation, fracture distribution, and flow focusing at the Nopal I location are presented below.

4.1. Precipitation and seepage

Results from the instrumented seepage collection columns within the back adit area indicate that seepage for individual collection sites varies temporally and spatially, and is strongly influenced by the timing and magnitude of precipitation. Of the six instrumented collection sites within the back adit, three (18A, 8C, and to a lesser degree, 3C) experienced high volumes of seepage (>300 ml within 12 hours) after one or more of the three large (>20 mm/day) precipitation events that occurred during the summer of 2006 (Fig. 7).

In addition to these high-volume flow events recorded in these locations occurring immediately following periods of large rainfall, there is a pattern of general seepage that appears to be spatially variable and seasonally controlled. Because of the presence of a summer monsoon period and a dry winter season (Fig. 5), infiltration of water at the surface is mostly restricted to the months of June to September. There is a time lag of weeks to months between the onset of the rainy season and the first appearance of seepage in many of the adit collectors. After seasonal seepage is initiated in the adit, seepage rates appear to be quite uniform over sustained periods, and then seepage diminishes to either very low levels or ceases altogether until the next year's seepage event begins. There is a general trend (see Fig. 7) towards earlier water arrival times in the back adit (Frame 1-3) and later arrival times in the front adit (Frame 4). This may be influenced by an increase in rock alteration and the presence of shorter average fracture lengths within the U orebody (Pearcy 1993), which could result in lower fracture network permeability for the front adit region. Although there was no collection instrumentation in the front adit location, the absence of seepage water in all but one of the collectors during the June-August 2006 collection period (when two of the three large precipitation events occurred) at this site (Fig. 7) suggests that this area does not have any active fast flow paths.

4.2. Evaporation and condensation

Evaporation occurring within the rock mass and in the drift likely plays a significant role in the overall trend of lower seepage volumes observed in the front adit locations. Continuous temperature and relative humidity data recorded by the weather station at the +10 level and instruments in the back adit are shown in Fig. 8. Although there was no continuous monitoring of the relative humidity and temperature levels for the front adit area, short-term environmental measurements conducted while

working in this portion of the adit are also plotted in Fig. 9. These data suggest that the proximity of the front adit collectors to the adit entrance likely resulted in increased evaporation of water from the adit walls. This would explain the lower seepage volumes collected throughout this area, especially during the hotter summer months when no seepage was observed in the front adit (Fig. 6). Seepage samples collected from the front adit had higher salinities and $^{18}\text{O}/^{16}\text{O}$ and D/H values than those from the back adit (unpublished data), consistent with evaporation being an important process in the front adit. Some of the collected volumes may have been affected by evaporation from the collection bottles or columns. However, this effect appears to have been minor, as only rarely did water levels in partially filled bottles that were left in the adit show any decrease in volume.

In the back adit area, where temperature, relative humidity, and barometric pressure values were monitored continuously, temperatures were stable and moderate (15-19°C) and relative humidity levels were quite high (> 85%) throughout the seepage collection period (Fig. 8), which would prevent much evaporative loss from occurring; this is in contrast with the large variations in outside temperature and the much lower relative humidity values in this arid environment. The restricted hose connection between the collection vessel and the seepage trays also limited evaporative loss. This would not have been the case for the plastic sheets that were originally used in collecting seepage samples for previous studies.

To establish quantitative relationship between location of seepage and seepage timing, we plotted the fraction of the seepage collected during the rainy season (November 2005, August 2006, and December 2006) against distance from the adit entrance in Fig. 9. This plot shows that approximately half of seepage in areas closer to the outside environment (Frames 3 and 4) occurs after the rainy season is over. In contrast, nearly all of the seepage at the innermost frame (Frame 1) occurs within the rainy season.

Field studies and modeling work conducted by Ghezzehei et al. (2004) indicate that the effects of evaporation are minimal for seepage into cavities when elevated (>85%) relative humidity conditions are present. Ghezzehei et al. (2004) also found that evaporation from cavity walls significantly reduces seepage in tests conducted under ventilated conditions at Yucca Mountain, where relative humidity fluctuated between 20% and 95%. In some portions of their study site, seepage was completely halted when relative humidity values dropped below 40%.

During times of elevated seepage (and thus, elevated humidity within the adit), condensation droplets were often observed on the outside of the seepage trays and collection bottles. To evaluate the potential for condensed water contributing to the water collected in the seepage trays, a separate condensate tray was installed in the back adit, with a Lexan roof mounted above it so that water could not drip directly into the collection tray. This collector was placed in a portion of the back adit where abundant condensate had been observed previously, and where a set of pressure-temperature sensors deployed adjacent to site 25A was rendered inoperative as a result of condensation affecting the electronics of the sensors. No condensate was found in the tray during the time when seepage was not occurring in this portion of the adit, but a significant amount (≥ 135 ml) of water was observed in the condensate collector for one time interval where seepage was extensive in this portion of the adit (August-December, 2006). Thus, a fraction of the collected “seepage” water may result from local condensation dripping down from the roof or occurring directly within the collection trays in certain regions of the adit. However, the original source of both seepage and condensate water is likely to be from precipitation that has infiltrated through the rock mass above the adit.

4.3. Fractures and seepage

Within the +00 adit at Nopal I, there are abundant steeply dipping fractures within the adit (Fig. 4). Initial modeling of infiltration and seepage as occurring through a series of planar, vertical fractures was conducted to evaluate flow transit times and seepage rates (Ghezzehei et al. 2006). Using a range of fracture apertures and frequencies, and assuming no fracture-matrix interaction (which would retard the flow of fluid movement), infiltration through the 8 m high vertical fracture system and seepage into the adit were predicted to occur within 24 hours after a 6 hour rainfall event. This result is consistent with the observations for the few instrumented locations where fast flow paths were observed, but contrasts with the long (1-6 month) time lags in seepage observed at many of the collection locations at the Nopal I study site.

While fractures are present throughout the rock mass at Nopal I (Fig. 4), only certain fractures appear to serve as primary flow paths for water traveling from the ground surface to the adit collectors. Many of the fractures have mineral coatings, suggesting that they have been sites for flow and transport. The presence of roots along some of the fractures in the +00 adit indicates that there are continuous

fracture pathways that connect the adit with the surface. Moreover, the arrival of large volumes of seepage water in three of the instrumented collector sites occurring in less than 4 hours following large (>20 mm/day) rain events suggests the existence of fast flow paths that appear to be linked to fractures. There are two large mapped fractures that intersect above the 18A collector, two parallel fractures that cut across the ceiling above the 8C collector, and another set of parallel fractures that go through the edge of the 3C collector area. A mapped fault cuts above a portion of the 30D collector (this fault is also seen exposed on the +10 surface), but this feature does not appear to contribute to the fast flow of water into the adit, as the neighboring collectors where this feature is also present also lack evidence for high-volume fluid flow. There were no long fractures above the 24B collector, consistent with the absence of fast-flow seepage in this area.

In Fig. 10, the fraction of seepage occurring during the rainy season is plotted against fracture density. These data represent the average seepage fraction and fracture density values for each row (five collectors). To distinguish the effect of fracture density from that of location within the adit (see section 4.2 and Fig. 9), the results of the four frames are plotted separately. Within each frame, where the effect of evaporation is approximately uniform, fast seepage fraction is positively correlated with fracture density (except in Frame 1). In Frame 1, where >90% of the seepage arrives during the rainy season, a weak negative correlation was detected between fracture density and fast seepage fraction. These observations suggest that high fracture density may be associated with high fracture connectivity, thereby resulting in fast flow pathways.

The distinct flow behavior observed for each of the individually instrumented seepage sites (Fig. 7) indicates that seepage is heterogeneous both temporally and spatially. The observed link between seasonal rainfall events and the onset of seepage suggests that the saturation levels of both fractures and matrix within the vadose zone that lead to seepage are controlled by the amount of infiltration that occurs following each precipitation event. While fractures are likely to serve as the primary conduits for fluid flow within the rock mass, the location, timing, and volumes of seepage may be influenced by other factors, such as surface flow, flow focusing, and flow diversion.

4.4. Surface flow and flow focusing

Although active seepage was not observed in the adit during our visits to the site, we did see features on the ceiling of the adit that appear to serve as drip points. These features often exhibited white mineralization with drops of water, and were located either near fractures or on low-lying points along the roof. The mined surface of the adit was quite uneven, so film flow along the ceiling could help focus seepage collection to these lower hanging features. In contrast, the one area in the back adit where the ceiling was elevated, forming a nave about 90 cm high, had some of the lowest observed seepage rates in the back adit (see row 24 in Fig. 7 and collector 24B in Fig. 7).

4.5. Flow diversion

The concept of a flow diversion around mined excavations in the unsaturated zone resulting from capillary barrier effects has been postulated as a potential process that would reduce seepage (Philip et al. 1989; Houseworth et al. 2003). Seepage within the adit is distributed in a very heterogeneous fashion, with mapped fractures and faults appearing to be related to zones of elevated seepage. There were two distinct collection regions within the adit where seepage was limited in volume. The first is the front adit area (Figs. 7d and 8), which is close to the adit entrance, where lower humidity and higher temperatures would result in greater evaporative loss from the rock mass, and thus lower seepage volumes. The second area where total seepage volumes were greatly reduced was in the back end of the back adit (Figs. 7a and 8). This site would be expected to have the least impact from evaporation, as it is furthest from the adit entrance. However, this is the one area where there are three walls (two sides of the adit, and the rear of the adit) where capillary flow diversion could occur, making it the one location where this effect would be expected to be strongest.

5. Conclusions

The following observations and interpretations can be made from the results of our seepage study.

1. Observed seepage volumes and arrival times in the Nopal +00 mine adit were highly heterogeneous. However, the largest seepage volumes occurred in the back adit during and just following the rainy season.

2. Seepage rates and arrival times were much lower/longer than those predicted by a simple planar fracture model (Ghezzehei et al. 2006) for most collection locations, suggesting that flow paths are complex. A few flow paths in the back adit carried large volumes of water, with large volumes of seepage occurring between July and November 2005 and again during the summer monsoon period between July and September of 2006. These seepage episodes are directly correlated with large rainfall events, and are likely associated with major fractures.
3. Most of the remaining portions of the front and back adit exhibited slow, steady seepage that begins after the start of the rainy season and persists for 4-6 months.
4. The arrival of the gradual seasonal seepage pulse occurred earlier in the back adit than in the front adit. This distribution of seepage vs. time could be due to the greater residual saturation in the back adit relative to the front adit, in accordance to lower evaporation and higher relative humidity factors previously discussed, as well as differences in the fracture-matrix flow pathways.
5. Condensation occurred within portions of the adit and contributed to the overall volume of "seepage" water collected within the adit.

These observations indicate that even a relatively thin (8 m) rock mass can exert a noticeable damping effect on infiltration, and that flow and transport models must incorporate fracture flow heterogeneity. Our general model is that for the Nopal I site, there is a seasonal pulse of infiltration associated with the rainy season. For areas with fast flow paths, there are punctuated large-flow events associated with episodes of heavy precipitation. Based on these field observations, it appears that there is a threshold amount of rain (> 20 mm/day) that is necessary to trigger such a flow event and overcome the seepage threshold for fractures that intersect the adit. These punctuated flow events are accompanied by a slower, more gradual pulse of infiltrating water that moves through the 8 m thick rock mass over a period of 1-6 months, with a much longer (3-6 month) flow duration. Seepage is also affected by evaporation (particularly in the front adit area) and condensation of water vapor within portions of the adit.

Matrix permeability of the Nopal tuff is extremely low, with measured values ranging from 0.001 to 0.098 md (Meyer 1995; Dobson et al. 2008). Thus, most of the flow is likely to be focused through the

fracture network. There is a similar density of fractures within and outside of the Nopal ore deposit (Leslie et al. 2005), but fractures within the U orebody are generally shorter in length (Pearcy 1994) and appear to have more extensive mineralization, resulting in lower fracture permeability, which may explain why no fast flow paths were observed in the front adit area.

Infiltration of precipitation, heterogeneous fluid flow through fractures and matrix in unsaturated tuffs, and the existence of fast flow paths are key components of flow and transport process models for Yucca Mountain (e.g., Wang et al. 1999; Flint et al. 2001a, b; Bodvarsson et al. 2003; Liu et al. 2003; Bagtzoglou and Cesano 2007b). Enhanced fluid flow in regions containing high permeability faults and fractures could increase the opportunity for transport of dissolved constituents in these areas.

However, there are a number of differences between Yucca Mountain and the Nopal I analogue that should be considered when applying the observations and conclusions reached in our study to Yucca Mountain. Current rainfall at Nopal I (~300 mm/y) is significantly higher than at Yucca Mountain (177 mm/y; Sharpe 2007). Rain at Nopal I is intercepted by a flat surface that is unlikely to produce significant runoff, which would not be the case on the rugged slopes of Yucca Mountain. Rainwater at Nopal is transported through a relatively thin layer (8 m) of fractured tuff that has no overlying soil horizon, whereas at Yucca Mountain water would pass through a thick (~300 m) unsaturated zone prior to reaching the proposed repository horizon. In addition, the unsaturated zone at Yucca Mountain contains a layer of nonwelded and relatively unfractured porous tuff (nonwelded Paintbrush tuff) in between several layers of fractured tuff, which would serve to redistribute water flow and perhaps reduce flow heterogeneity (Flint et al. 2001b). At Nopal I, some of the observed fractures extend from the ground surface down to the +00 adit, providing direct and rapid pathways for percolation waters. While similar fast flow features have been documented at Yucca Mountain (Flint et al. 2001b; Campbell et al. 2003), it is likely that they are less abundant, and primarily restricted to areas near major faults. The presence of the open fractures at Nopal I is likely responsible for the highly heterogeneous (in space and time) seepage patterns observed at Nopal I.

Acknowledgments

This work was supported by the U.S. Department of Energy Contract No. DE-AC02-05CH11231. The United States Government retains and the publisher, by accepting the article for publication, acknowledges that the United States Government retains a non-exclusive, paid-up, irrevocable, world-wide license to publish or reproduce the published form of this manuscript, or allow others to do so, for United States Government purposes. The views and opinions of authors expressed in this article do not necessarily state or reflect those of the United States Government or any agency thereof or The Regents of the University of California. Ardyth Simmons (LANL) was instrumental in initiating the Peña Blanca natural analogue project, and Schön Levy (LANL) provided helpful oversight during later stages of the project. John Dinsmoor and Alan Mitchell (LANL) ensured that our field study was conducted safely and provided helpful logistical support. Phil Goodell (UTEP), Ignacio Reyes (UACH), and Mostafa Fayek (U. Manitoba) shared useful insights about the Nopal I deposit. Tim Kneafsey (LBNL), Stefan Finsterle (LBNL), George Saulnier (Areva), and Amvrossios Bagtzoglou (UConn) provided us with helpful reviews of this work. We thank Victor Reyes (Centro de Investigación sobre Sequía, Instituto de Ecología, A.C.) for his support of our field study and Alba Luz Saucedo and Octavio Hinojosa for their assistance in the field. We also thank Ing. Alejandro González Serratos (Servicio Meteorológico Nacional) for providing us with historical meteorological data for the now-defunct Los Pozos weather station.

6. References

- Abelin H, Birgersson L, Gidlund J, Neretnieks I (1991) A large-scale flow and tracer experiment in granite
1. Experimental design and flow distribution. *Water Resour Res* 27:3107–3117
- Abelin H, Birgersson L, Moreno L, Widen H, Agren T, Neretnieks I (1991) A large-scale flow and tracer experiment in granite
2. Results and interpretation. *Water Resour Res* 27:3119–3135
- Bagtzoglou AC, Cesano D (2007a) Dripping into unsaturated rock underground excavations – literature review and geologic and hydrogeologic setting description. *Environ Geol* 51:1285–1294
- Bagtzoglou AC, Cesano D (2007b) Dripping into unsaturated rock underground excavations: model testing at the Yucca Mountain exploratory studies facility. *Environ Geol* 51:1295–1306
- Bodvarsson GS, Wu Y-S, Zhang K (2003) Development of discrete flow paths in unsaturated fractures at Yucca Mountain. *J Contam Hydrol* 62-63:23–42

- Calas G, Agrinier P, Allard T, Ildefonse P (2008) Alteration geochemistry of the Nopal I uranium deposit (Sierra Peña Blanca, Mexico), a natural analogue for a radioactive waste repository in volcanic tuffs. *Terra Nova* 20:206–212
- Campbell K, Wolfsberg A, Fabryka-Martin J, Sweetkind D (2003) Chlorine-36 data at Yucca Mountain: statistical tests of conceptual models for unsaturated-zone flow. *J Contam Hydrol* 62-63:43–61
- Davidson GR, Bassett RL, Hardin EL, Thompson DL (1998) Geochemical evidence of preferential flow of water through fractures in unsaturated tuff, Apache Leap, Arizona. *Appl Geochem* 13:185–195
- Dobson PF, Fayek M, Goodell PC, Ghezzehei TA, Melchor F, Murrell MT, Oliver R, Reyes-Cortés IA, de la Garza R, Simmons A (2008) Stratigraphy of the PB-1 well, Nopal I uranium deposit, Sierra Peña Blanca, Chihuahua, Mexico. *Int Geol Rev* 50:959–974
- Fayek M, Ren M, Goodell P, Dobson P, Saucedo A, Kelts A, Utsunomiya S, Ewing RC, Riciputi LR, Reyes I (2006) Paragenesis and geochronology of the Nopal I uranium deposit, Mexico. In: *Proc 2006 Int High Lev Radioact Waste Manag Conf*, Las Vegas, NV, Am Nucl Soc:55–62
- Finsterle S (2000) Using the continuum approach to model unsaturated flow in fractured rock. *Water Resour Res* 36:2055–2066
- Flint AL, Flint LE, Bodvarsson GS, Kwicklis EM, Fabryka-Martin J, (2001a) Evolution of the conceptual model of unsaturated zone hydrology at Yucca Mountain, Nevada. *J Hydrol* 247:1–30
- Flint AL, Flint LE, Kwicklis EM, Bodvarsson GS, Fabryka-Martin JM (2001b) Hydrology of Yucca Mountain, Nevada. *Rev Geophys* 39:447–470
- Ghezzehei TA, Dobson PF, Rodriguez JA, Cook PJ (2006) Infiltration and seepage through fractured welded tuff. In: *Proc 2006 Int High Lev Radioact Waste Manag Conf*, Las Vegas, NV, Am Nucl Soc:105–110
- Ghezzehei TA, Trautz RC, Finsterle S, Cook PJ, Ahlers CF (2004) Modeling coupled evaporation and seepage in ventilated cavities. *Vadose Zone J* 3:806–818
- Goldstein SJ, Luo S, Ku TL, Murrell MT (2006) Uranium-series constraints on radionuclide transport and groundwater flow at the Nopal I uranium deposit, Sierra Peña Blanca, Mexico. In: *Proc 2006 Int High Lev Radioact Waste Manag Conf*, Las Vegas, NV, Am Nucl Soc:215–222

- Goldstein SJ, Abdel-Fattah AI, Murrell MT, Dobson PF, Norman DE, Amato RS, Nunn AJ (2010) Uranium-series constraints on radionuclide transport and groundwater flow at the Nopal I uranium deposit, Sierra Peña Blanca, Mexico. *Environ Sci Tech* 44:1579–1586
- Green RT, Rice G (1995) Numerical analysis of a proposed percolation experiment at the Peña Blanca natural analog site. In: *Proc 1995 Int High Lev Radioact Waste Manag Conf, Las Vegas, NV, Am Nucl Soc*:226–228
- Houseworth JE, Finsterle S, Bodvarsson GS (2003) Flow and transport in the drift shadow in a dual-continuum model. *J Contam Hydrol* 62-62:133–156
- Ku TL, Luo S, Goldstein SJ, Murrell MT, Chu WL, Dobson PF (2009) Modeling non-steady state radioisotope transport in the vadose zone – A case study using uranium isotopes at Peña Blanca, Mexico. *Geochim Cosmochim Acta* 73:6052–6064
- Leslie BW, Smart KJ, Percy EC (2005) Characterization of fractures at the Nopal I site and comparison to fracture characteristics of Yucca Mountain, Nevada. *Geol Soc Am Abstr with Progr* 37(7):196
- Levy S, Goldstein S, Dobson PF, Goodell P, Ku T-L, Abdel-Fattah A, Saulnier G, Fayek M, de la Garza R (2011) Peña Blanca natural analogue project: Summary of activities. In: *Proc 2011 Int High Lev Radioact Waste Manag Conf, Albuquerque, NM, Am Nucl Soc*: 330-341.
- Liu HH, Doughty C, Bodvarsson GS (1998) An active fracture model for unsaturated flow and transport in fractured rocks. *Water Resour Res* 34:2633–2646
- Liu HH, Haukwa CB, Ahlers CF, Bodvarsson GS, Flint AL, Guertal WB (2003) Modeling flow and transport in unsaturated fractured rock: an evaluation of the continuum approach. *J Contam Hydrol* 62-63:173–188
- Meyer KA (1995) Hydraulic characterization of hydrothermally altered Nopal tuff. M.S. Thesis, University of Texas at San Antonio
- Murphy WM (2002) Peña Blanca and Yucca Mountain: An introduction. In: von Maravic H, Alexander WR (eds) *Eighth EC Natural Analogue Working Group Meeting, EUR 19118 EN, European Commission, Directorate-General for Research, Luxembourg*:315–320
- Murphy WM, Pickett DA, Percy EC (2002) Peña Blanca natural analog data in recent performance assessment models for the proposed geologic repository at Yucca Mountain, Nevada. In: von

- Maravic H, Alexander WR (eds) Eighth EC Natural Analogue Working Group Meeting, EUR 19118 EN, European Commission, Directorate-General for Research, Luxembourg:365–375
- Paces JB, Neymark LA, Marshall BD, Whelan JF, Peterman ZE (1998) Inferences for Yucca Mountain Unsaturated-Zone Hydrology from Secondary Minerals In: Proc Ninth Int High Lev Radioact Waste Manag Conf, Las Vegas, NV, Am Nucl Soc:36–39
- Pearcy EC (1994) Fracture transport of uranium at the Nopal I natural analog site. CNWRA 94-011. San Antonio, Texas, Center for Nuclear Waste Regulatory Analyses
- Pearcy EC, Prikryl JD, Leslie BW (1995) Uranium transport through fractured silicic tuff and relative retention in areas with distinct fracture characteristics. *Appl Geochem* 10:685–704
- Philip JR, Knight JH, Waechter RT (1989) Unsaturated seepage and subterranean holes: conspectus, and exclusion problem for circular cylindrical cavities. *Water Resour Res* 25:16–28
- Pickett DA, Murphy WM (1999) Unsaturated zone waters from the Nopal I natural analog, Chihuahua, Mexico—Implications for radionuclide mobility at Yucca Mountain. In: Wronkiewicz DJ, Lee JH (eds), *Sci Basis for Nucl Waste Manag XXII, Symp Proc 556*, Materials Res. Soc., Warrendale, PA:809–816
- Prikryl JD, Pickett DA, Murphy WM, Pearcy EC (1997) Migration behavior of naturally occurring radionuclides at the Nopal I uranium deposit, Chihuahua, Mexico. *J Contam Hydrol* 26:61–69
- Reyes-Cortés IA (1997) Geologic studies in the Sierra de Peña Blanca, Chihuahua, México. Ph.D. diss University of Texas at El Paso
- Reyes-Cortés IA (2002) Geologic setting and mineralization: Sierra Peña Blanca, Chihuahua, México. In: von Maravic H, Alexander WR (eds) Eighth EC Natural Analogue Working Group Meeting, EUR 19118 EN, European Commission, Directorate-General for Research, Luxembourg:321–331
- Saulnier GJ Jr, Statham W (2006) The Peña Blanca Natural Analogue Performance Assessment Model. In: Proc 2006 Int High Lev Radioact Waste Manag Conf, Las Vegas, NV, Am Nucl Soc:228–235
- Sharpe SE (2007) Using modern through mid-Pleistocene climate proxy data to bound future variations in infiltration at Yucca Mountain. In: Stuckless JS, Levich RA (eds) *The geology and climatology of Yucca Mountain and vicinity, southern Nevada and California*. *Geol Soc Am Mem* 119:155–205

- Shimajima E, Tanaka T, Yoshioka R, Hosono Y (1993) Seepage into a mountain tunnel and rain infiltration. *J Hydrol* 147:121–151
- Simmons AM, Murrell MT, Goldstein SJ (2002) Seasonal fluctuation in uranium decay-series composition of waters at Peña Blanca, Mexico. *Geol Soc Am Abstr with Progr* 34, paper 103-6
- Simmons AM, Stuckless JS (2010) Analogues to features and processes of a high-level radioactive waste repository proposed for Yucca Mountain, Nevada. USGS Prof Paper 1779
- Trautz RC, Wang JSY (2002) Seepage into an underground opening constructed in unsaturated rock under evaporative conditions. *Water Resour Res* 38:1188, doi:10.1029/2001WR000690
- Wang JSY, Trautz RC, Cook PJ, Finsterle S, James AL, Birkholzer J (1999) Field tests and model analyses of seepage into drift. *J Contam Hydrol* 38:323–347

Figures

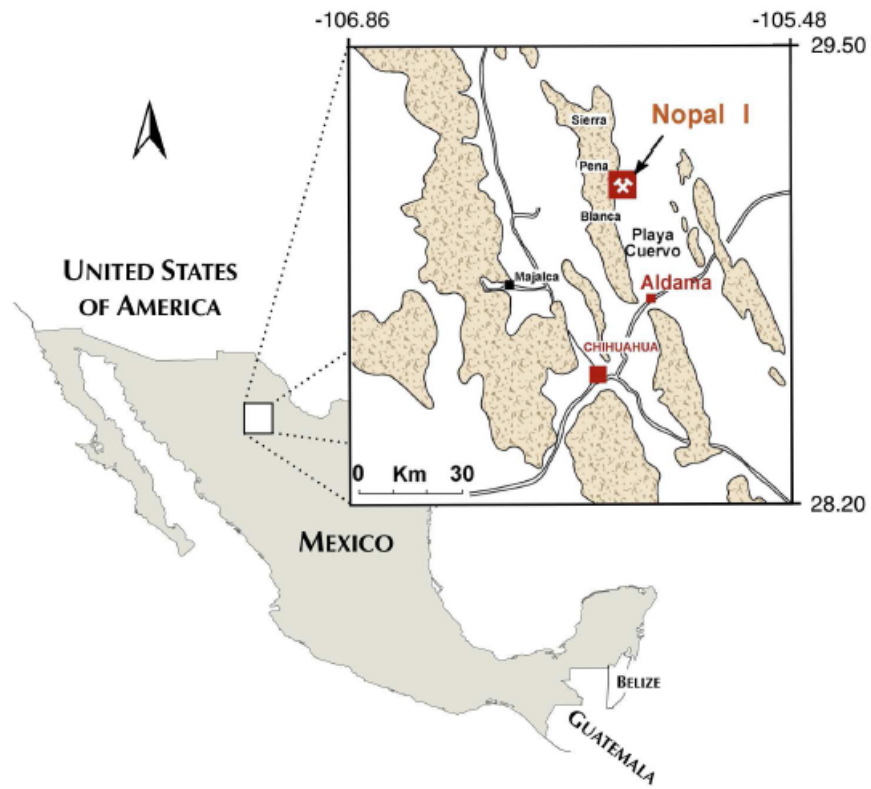


Fig. 1 Location map of Nopal I uranium mine, Chihuahua, Mexico



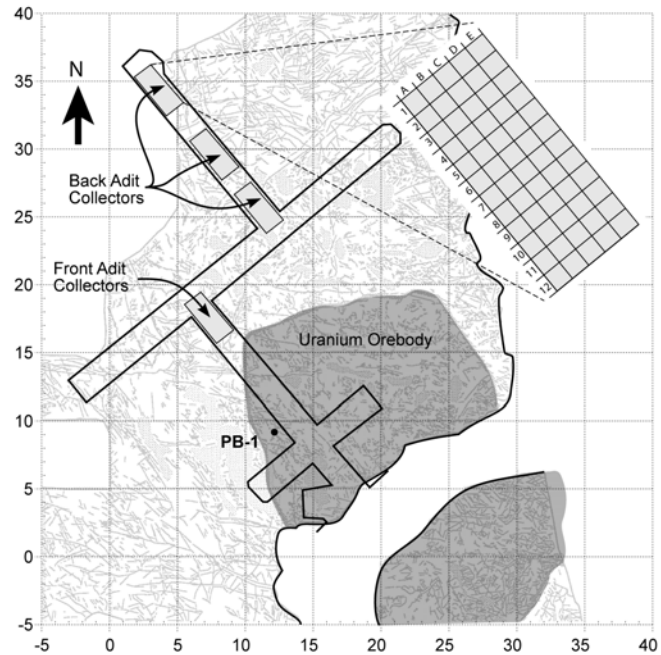


Fig. 2 (a) View of +10 level of Nopal I mine, where infiltration of rainwater occurs. Entrance to +00 adit is located just below and left of PB-1 wellhead (yellow cement feature in left center portion of photo). Nopal weather station is located on +20 level just above PB-2 well. (b) Plan view map of the Nopal I uranium deposit, indicating the location of the +00 adit, the seepage collector arrays (with a depiction of the array numbering system), and the PB-1 well. The locations of mapped fractures and U orebody are from Percy et al. (1995). Grid divisions are in meters. The Nopal I weather station is located ~63 m WSW of the PB-1 well



Fig. 3 Array of collection bins and instrumented collection columns (sites 24C, 18A, 8C, and 3C, from foreground to background) within adit seepage collection system

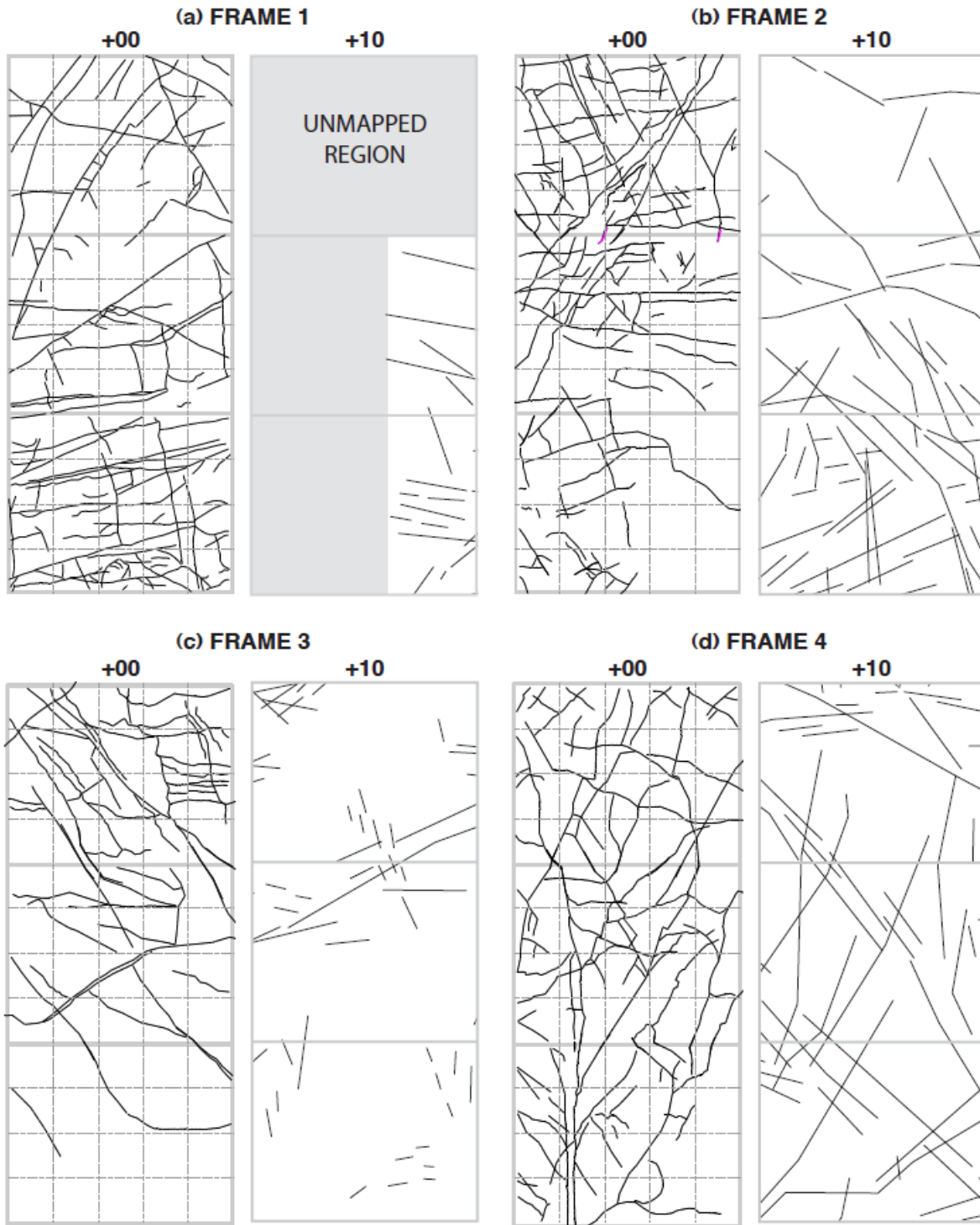


Fig. 4 Fracture map of adit roof (plan view projection) over the four seepage collection frames in the back and front portions of the +00 m adit and fractures from the corresponding locations on the +10 level (surface fracture data from Percy et al., 1995 and Reyes-Cortés, 1997). Each collection frame covers

an area measuring 1.5 m by 3.6 m. Individual bins within collection trays mounted within the frames collect seepage water over an area of 915 cm². Locations of collection frames shown in Fig. 2. The labels +00 and +10 denote adit ceiling and +10 level ground surface, respectively

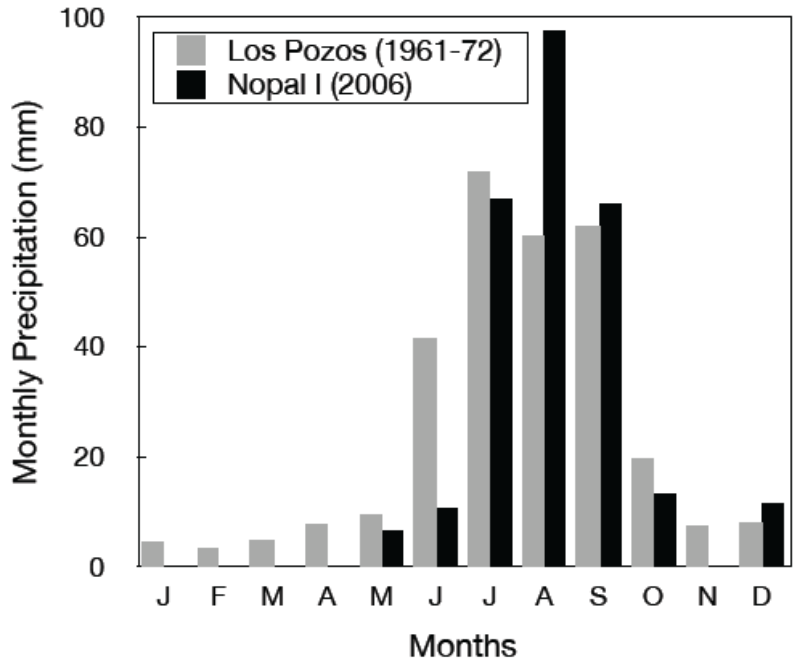


Fig. 5 Average rainfall, Los Pozos, Chihuahua (29° 05' 03" N, 105° 58' 02" W, 1200 masl; 1961-1972 data from Servicio Meteorológico Nacional — station 08179) and Nopal I weather station, Chihuahua (29° 06' 41" N, 106° 02' 09", 1476 masl), 2006 data (data recorded from Mar. 20 until Dec. 14, 2006)

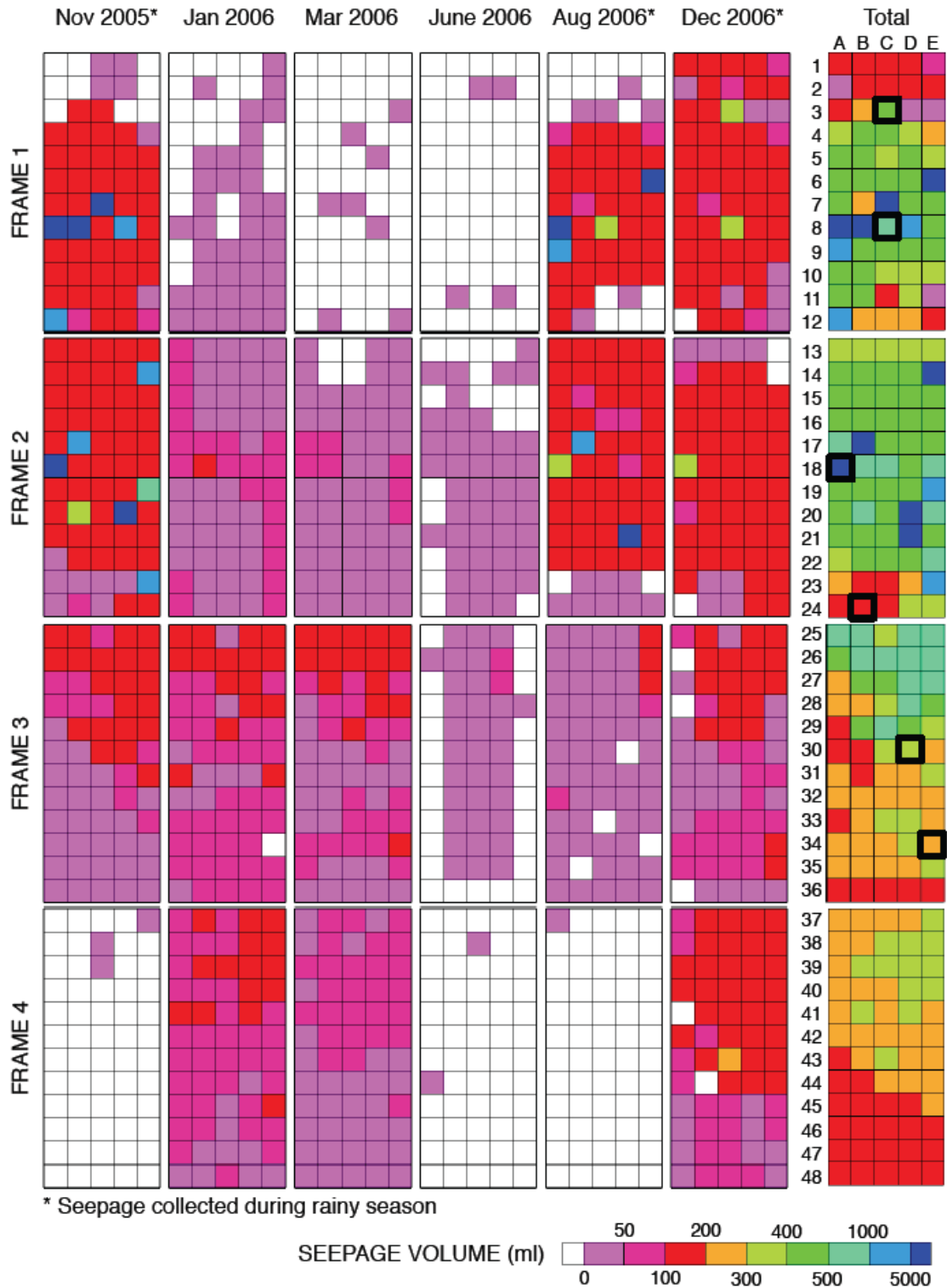


Fig. 6 Seepage amounts between visits for collectors. The highlighted boxes indicate the location of automated seepage collectors. Absence of seepage in bottles in some of the edge collection locations of Frames 2 and 3 for June 2006 visit caused by thirsty animal in adit draining bottles. The last column

reflects cumulative seepage amounts collected for each station between installation of seepage collection system in April 2005 and final visit to site in December 2006

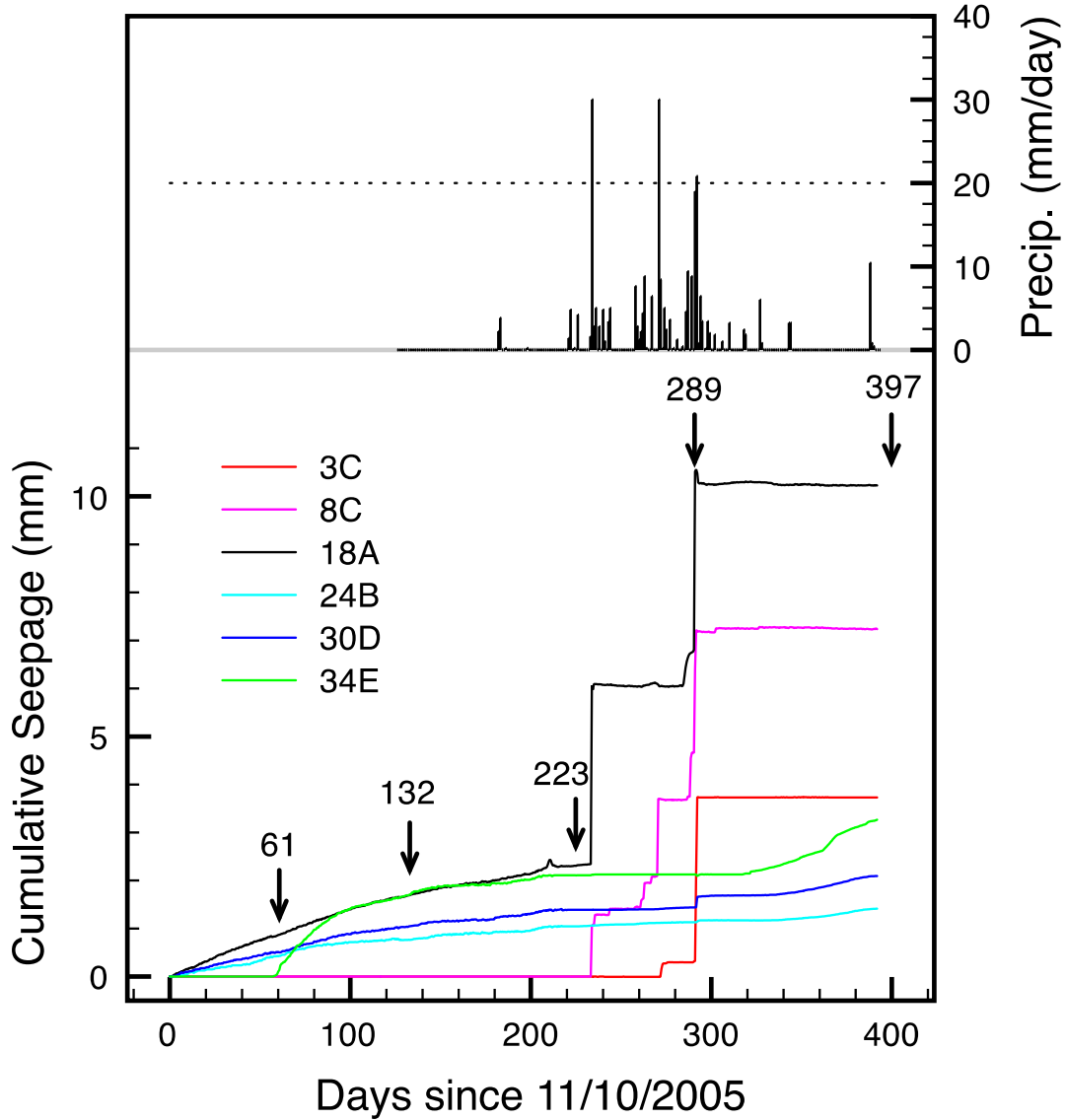


Fig. 7 Daily rainfall and measured seepage volumes for the Nopal I site. Note that steps in seepage amounts represent filling of 340 ml collector column volume, and thus these plots (in the case of collectors 3C, 8C, and 18A) represent minimum seepage volumes. Seepage collection in 34E did not begin until January 2006 (Day 61). Arrows indicate days when seepage was collected in the adit

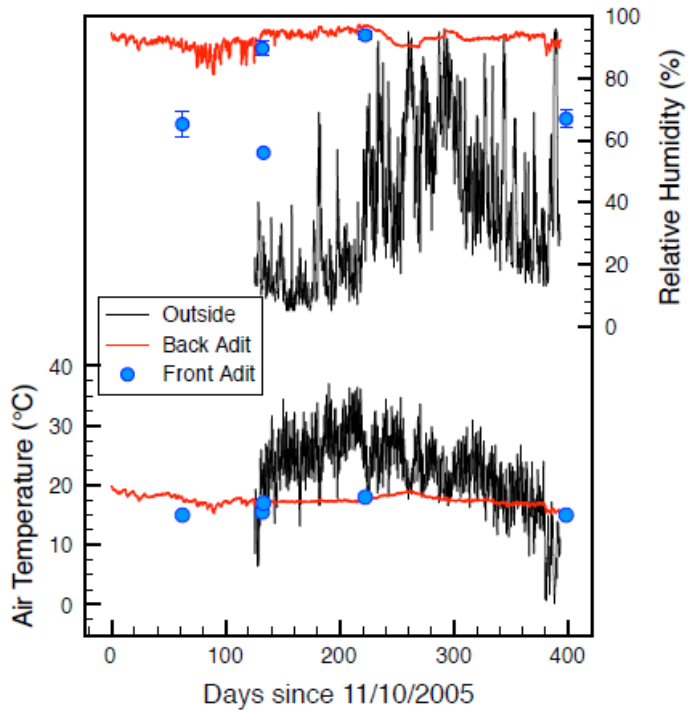


Fig. 8 Measured temperature and relative humidity values from the Nopal I weather station (outside), the back portion (Row 1) of the +00 adit (back adit), and short-term records during site visits in the front adit

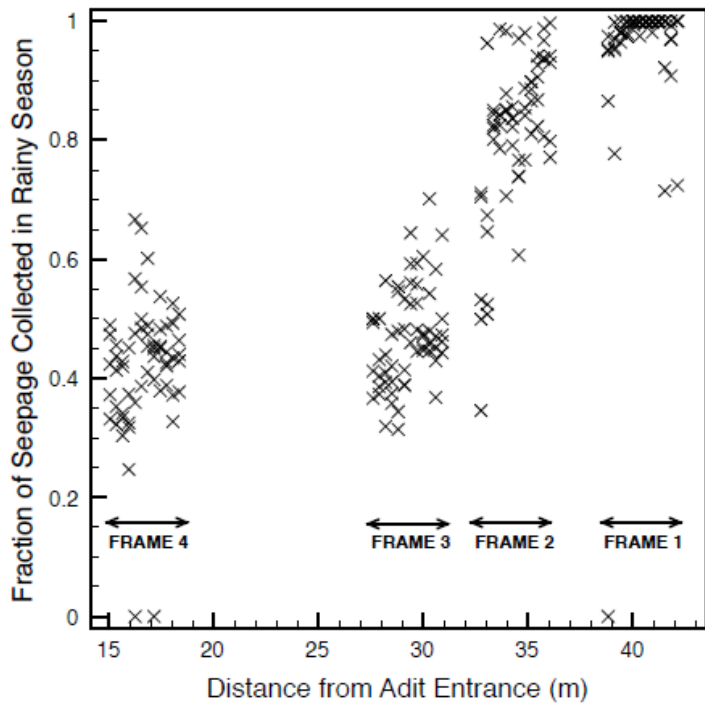


Fig. 9 Relation between fraction of seepage occurring during rainy season (fast seepage) and distance from the adit entrance

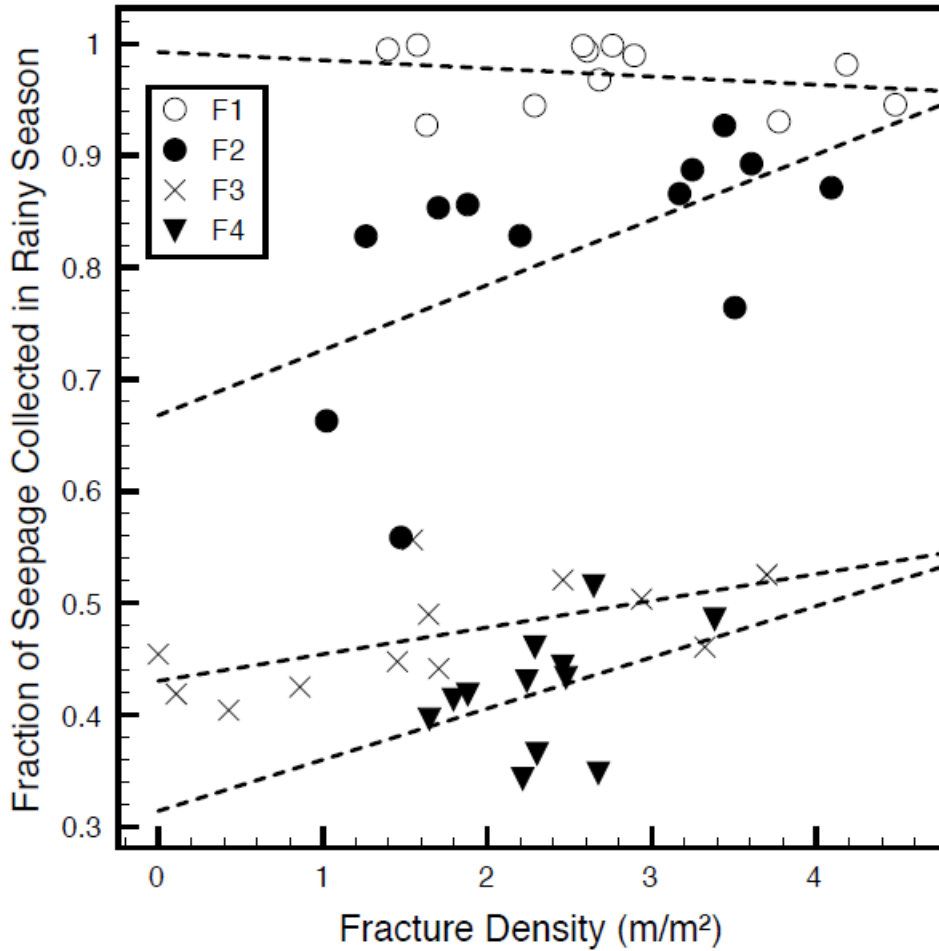


Fig. 10 Relation between fraction of seepage occurring during rainy season (fast seepage) and fracture density (m/m²). Values averaged by row and plotted with separate symbols for each frame. Coefficients of linear correlation between fracture density and fast seepage fraction are -0.25, 0.58, 0.61, and 0.40 and regression r-square values are 0.06, 0.34, 0.38, and 0.16 for frames 1 through 4, respectively

DISCLAIMER

This document was prepared as an account of work sponsored by the United States Government. While this document is believed to contain correct information, neither the United States Government nor any agency thereof, nor The Regents of the University of California, nor any of their employees, makes any warranty, express or implied, or assumes any legal responsibility for the accuracy, completeness, or usefulness of any information, apparatus, product, or process disclosed, or represents that its use would not infringe privately owned rights. Reference herein to any specific commercial product, process, or service by its trade name, trademark, manufacturer, or otherwise, does not necessarily constitute or imply its endorsement, recommendation, or favoring by the United States Government or any agency thereof, or The Regents of the University of California. The views and opinions of authors expressed herein do not necessarily state or reflect those of the United States Government or any agency thereof or The Regents of the University of California.

Ernest Orlando Lawrence Berkeley National Laboratory is an equal opportunity employer.